Peer-reviewed version available at Sensors 2018, 18, 1623; doi:10.3390/s18051623

Article

Microfluidic cultivation and laser tweezers Raman spectroscopy of *E. coli* under antibiotic stress

Zdeněk Pilát[1,*], Silvie Bernatová[1], Jan Ježek[1], Johanna Kirchhoff[2,3,4], Astrid Tannert [2,4], Ute Neugebauer[2,3,4], Ota Samek[1] and Pavel Zemánek[1]

[1] Institute of Scientific Instruments (ISI) of the Czech Academy of Sciences, v.v.i., Kralovopolska 147, 612 64 Brno, Czech Republic.
[2] Center for Sepsis Control and Care (CSCC), Jena University Hospital, Am Klinikum 1, D-07747 Jena, Germany.
[3] Institute of Physical Chemistry, Friedrich Schiller University Jena, Helmholtzweg 4, D-07743 Jena, Germany.
[4] Leibniz Institute of Photonic Technology (Leibniz IPHT), Albert-Einstein-Str. 9, D-07745 Jena. Germany.
* Correspondence: pilat@isibrno.cz; Tel.: +420-541-514-521

Abstract: Analyzing the cells in various body fluids can greatly deepen the understanding of the mechanisms governing the cellular physiology. Because of the variability of physiological and metabolic states, it is important to be able to perform such studies on individual cells. Therefore, we developed an optofluidic system in which we precisely manipulated and monitored individual cells of *Escherichia coli*. We used laser tweezers Raman spectroscopy (LTRS) in a microchamber chip to manipulate and analyze individual *E. coli* cells. We subjected the cells to antibiotic cefotaxime, and we observed the changes by the time-lapse microscopy and Raman spectroscopy. We found observable changes in the cellular morphology (cell elongation) and in Raman spectra, which were consistent with other recently published observations. We tested the capabilities of the optofluidic system and found it to be a reliable and versatile solution for this class of microbiological experiments.

Keywords: Raman microspectroscopy; optical tweezers; optofluidics; *E. coli*; antibiotics

1. Introduction

Raman spectroscopy combined with laser tweezers (LTRS), together with a microfluidic chip that allows compartmentalization of a few or individual cells and highly controlled exchange of the cell suspension fluids, can form the basis of a system for cell micromanipulation and sorting [1, 2]. Raman spectroscopy is an analytical method that is based on detecting the vibrations of chemical bonds of molecules present in cells and nature in general, which makes it ideal for metabolomic analysis [3, 4] and fingerprinting [5, 6, 7]. After acquiring the spectrum from optically trapped cell, the data is analyzed and the cell can be subsequently sorted by an active micromanipulation with the optical trap [8, 9]. Properly implemented cell sorting is a completely non-invasive process and the sorted cells can be used for further cultivation and analysis [10, 11]. Furthermore, LTRS implemented in the microfluidic chip can serve to study the dynamics of the response of an individual cell to a controlled external stimulus or stress factor. This can be achieved by creating a concentration gradient and moving the studied cells into different compartments on the chip containing different antibiotic concentration and monitoring their response via Raman spectroscopy [12].

Microfluidic chips with cell incubation microchambers fabricated in ISI were used for our experiments. The design was optimized based on the previous experiences from their use and the experimental needs. We generated a laminar flow of cultivation medium in the chip, we loaded the bacterial cells, and then we used optical tweezers to transport these cells into the microchambers.

During the experiment, the cells were placed in these dedicated incubation microchambers to prevent them from moving away with the cultivation medium flow and to allow undisturbed acquisition of time-lapse images or Raman spectra. After the antibiotic was introduced into the medium flow, within a few seconds it freely diffused into the microchambers. Therefore, the concentration of the applied stress factor (antibiotic) at the cell location and the time of exposure of the cells to the stimulus was precisely defined.

New methods to characterize the antibiotic susceptibility of bacterial pathogens in short times are of utmost importance. In times of rising antibiotic resistances the known resistance pattern of a pathogen helps the treating physician to prescribe the right antibiotic therapy in time. Established antibiotic susceptibility testing in the clinical routine is based on time-consuming cultivation and the result is usually not obtained before one or sometimes even after two days. Emerging alternative methods, such as new methods based on polymerase chain reaction (PCR) are much faster, but also very costly. Raman spectroscopy as a label-free and non-invasive method holds high potential to advance fast antibiotic susceptibility testing. It was already shown that successful antibiotic-bacteria interaction can be probed after half an hour only [13] which can be utilized in a fast antibiotic susceptibility testing within only 3.5 hours [14, 15]. Furthermore, it can also be used to quantitatively determine the minimal inhibitory concentration [16].

The ultimate application of this technology to body fluids requires advanced microfluidic technology. Different approaches were already tested and implemented into a microfluidic device. Dielectrophoresis [17, 14] as well as centrifugal force [18] could successfully be applied to enrich the bacteria from urine samples. LTRS systems combined with microfluidic techniques offer furthermore the potential different to selectively remove cells from body liquids which are not targeted for analysis. We have developed several solutions in the area combining lasers and microfluidic environment [19, 20]. The chamber design was found to be quite successful for optical trapping experiments involving yeast cells [19] and currently we use it for experiments with *E. coli*. We aim to effectively combine microfluidics with our expertise in Raman analysis of bacteria and cells in general [21, 22, 23, 24, 25, 26, 27].

2. Materials and Methods

2.1. Optofluidic system

The layout of our specialized system for LTRS in microfluidic chip with microchambers is schematically depicted in Figure 1. We used it in combination with computer programmable syringe pumps (1-5 pumping units according to needs) which supply different liquids into the microfluidic micro-chamber chip, such as different media, buffers, antibiotics solutions, inoculum, etc. The microfluidic part of the system consisted of syringe pumps (NE1001, New Era Pump Systems, Inc., Farmingdale, NY, USA), 1 mL glass syringes (Hamilton, Bonaduz, Switzerland), luer-lock connectors (IDEX Health & Science LLC, Oak Harbor, WA, USA), and microfluidic tubing from the same manufacturer (PEEK, internal diameter 360 μm), which connected the chip to the syringe on one end of the main channel and to a waste container on the opposite end. In all the experiments, flow rate of the cultivation medium was set to 100 μL/h.

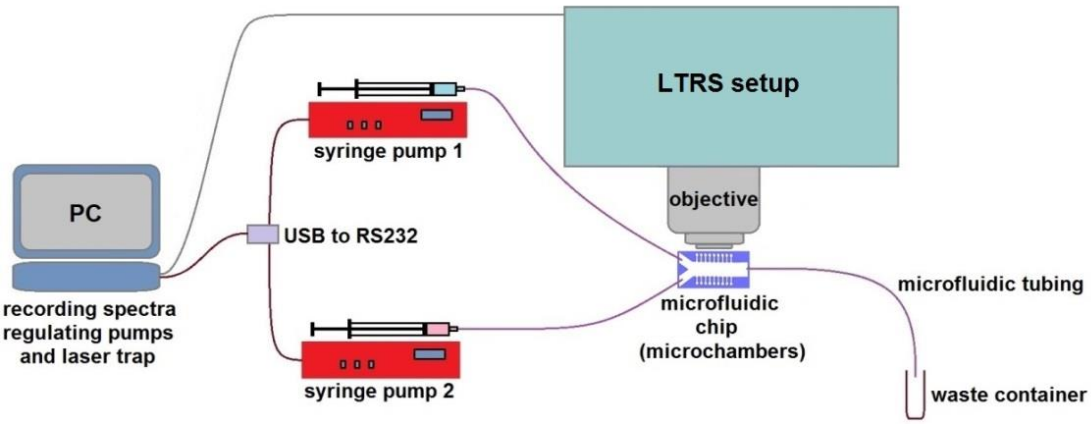

Figure 1. An optofluidic system for studying of individual living bacteria by laser trapping – Raman spectroscopy (LTRS) in microfluidic environment. The microfluidic chip with microchambers, under the microscope objective of the LTRS system, is interconnected with the syringe pumps that supply the cultivation medium and the tested antibiotic solution. The pumps and the LTRS system are regulated from dedicated software on a PC.

2.2. LTRS system

Main element of our optofluidic setup is the homemade laser tweezers – Raman spectroscopy (LTRS) system. This system was a modified version of the setup used by Bernatová *et al*. [24]. The schematic diagram of the LTRS setup is on Figure 2. It combines a Raman microspectrometer with optical tweezers [28, 29] providing spatial confinement of individual bacterial cells during Raman spectrum acquisition. The same laser beam is used for optical trapping and Raman spectroscopy. The output beam from a laser (output power ~0.5W, λ = 785 nm, Sacher Lasertechnik GmbH, Marburg, Germany) was delivered to the setup by an optical fiber and its diameter was expanded 3× by an external telescope (not shown in Figure 2.). From the telescope the beam passed through a bandpass filter BF (transmission bandwidth 3 nm centered on 785 nm; MaxLine LL01-785, Semrock, Rochester, NY, USA) to eliminate unwanted laser wavelengths. The power of the laser beam for Raman spectroscopy was roughly adjusted by a neutral density filter NDF1 and fine setting was done by a combination of a $\lambda/2$ wave plate WP and a polarizing beam splitter PBS. Beam diameter was further enlarged 2× by beam expander Exp. The laser beam was coupled to the microscope frame via a dichroic mirror D (LPD01-785RS, Semrock) and focused on the specimen with a water-immersion objective lens (UPLSAPO 60×, NA 1.20, Olympus, Tokyo, Japan). The maximal available laser power at the specimen plane was approximately 150 mW. The objective was mounted on a custom-made aluminium frame that also provided a stable support for the sample illumination path and 3-axis piezo-driven stage (P-517.3CL, Physik Instrumente, Karlsruhe, Germany) for positioning the sample relative to the beam focus. The Raman scattered light from the trapped microorganism was collected by the same water-immersion objective, focused by a lens L2 on the entrance slit of an imaging spectrograph (focal length 300 mm, f/3.9, 600 gr/mm diffraction grating, SpectraPro 2300i, PI Acton, Acton, MA, USA), imaged on the chip of a high-sensitivity liquid-nitrogen-cooled spectroscopic CCD camera (Spec-10:100BR/LN, Princeton Instruments, Acton, MA, USA), and recorded using the camera control software (WinSpec, Acton, MA, USA). Rayleigh scattered light at the laser wavelength was blocked by two edge filters NF1 (ZX000626, Iridian, Ottawa, Canada) and NF2 (LP02-785RS, Semrock) and did not enter the spectrograph.

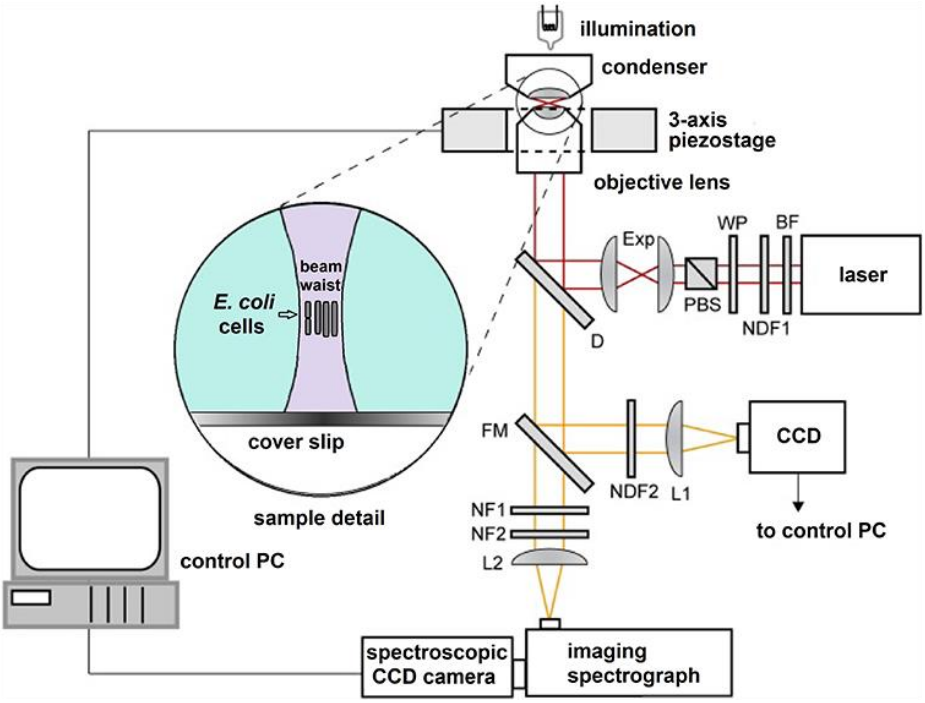

Figure 2. Schematic diagram of the LTRS setup where the same laser beam is used for optical trapping and Raman analysis. BF–band pass filter, D–dichroic mirror, Exp–beam expander, FM–flipping mirror, L1,2–lenses, NDF1,2–neutral density filters, NF1,2–edge filters, PBS–polarizing beam splitter, WP–lambda-half wave plate. Inset shows the detail of optically trapped bacteria near the focus of the laser beam. See details in the main text.

2.3. Microfluidic chips

Crucial element of the optofluidic system is the microfluidic chip. Our microfluidic chips were fabricated from poly(dimethyl)siloxane (PDMS) by conventional soft lithography, using master stamps based on negative SU-8 epoxy photoresist deposited on a silicon substrate [30, 19]. In brief, SU-8 was spin-coated on the silicon wafer, illuminated by a UV lamp through a mask, and developed. The masks for photolithographic patterning of SU-8 were fabricated by ink-jet printing on a transparent foil by a specialized company (Gatema, Brno, Czech Republic). PDMS mixture (base to curing agent ratio of 10:1) was then poured into a mold formed by the SU-8 master stamp on Si wafer at the bottom and a square frame machined from polycarbonate. After curing, the resultant PDMS device was peeled off from the mold and attached to a glass slide using standard oxygen plasma treatment.

The layout of microfluidic chips used in the experiments was previously employed [19] and is apparent from Figure 3. Individual sample chambers of cylindrical shape (diameter 20 μm or 25 μm) were connected to the wide main microfluidic channel (width 100 μm) by side channels of width 12 μm and length 60 μm. Height of all chambers and channels in the chip was 20 μm. Such configuration ensured that the cells could not escape easily from the chambers only due to their diffusion. On the other hand, the length of the side channels was sufficiently short to permit diffusion-mediated replenishment of nutrients in the chambers during the course of the experiment.

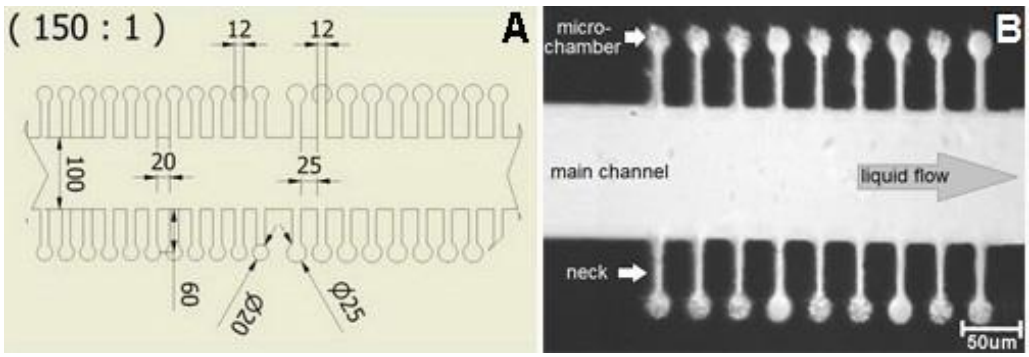

Figure 3. Microfluidic chamber chip used for *E. coli* cultivation, Raman spectroscopy and optical trapping experiments. A: A detail of the central part of the chip (dimensions in μm); B: A microscope image of individual micro-chambers in the chip and the adjacent main channel. The main channel in the center is connected with narrow necks to the microchambers. *E. coli* cells are present in most of the chambers, they appear dark and dot- or rod-shaped, depending on their positions. The main channel delivers fresh culture medium to the cells in the chambers. The nutrients from the medium and the products of bacterial metabolism diffuse through the neck in and out of the microchamber.

2.4. Bacterial samples: Strain and growth condition

In this study the patient isolate *E. coli* 683 was used. This strain originated from the blood of a sepsis patient and is part of the strain collection at the PathogenBiobank at the Institute of Medical Microbiology and the Center for Sepsis Control and Care of Jena University Hospital. Casein soya (CASO) medium (Sigma-Aldrich, sterilized by autoclaving for 15 min at 120 °C) was used for cultivation. A sample of bacteria was cultivated on a CASO agar plate, then transferred to liquid medium and incubated with shaking at 37 °C for 60 min before injection into the chip or off-chip cultivation with cefotaxime (2 mg/L in CASO medium). The cell count of the injected culture was in the order of 10^6 cells/mL. Small variations in the cell count of the injected culture had no influence on the experiment.

2.5. Optical trapping procedure

The procedure for optical trapping experiments with bacterial cells, similar to our previous experiments [19, 31] was as follows. First, the cell culture suspended in the CASO medium was introduced into the main microfluidic channel. Subsequently, all cells studied in a single experimental run were placed one-by-one into adjacent micro-chambers using low-power optical tweezers. In order to minimize the impact of optical trapping on the cells, we adjusted the laser power near the minimal effective trapping power (approx. 10 mW). In addition, this initial optical manipulation was carried out as quickly as possible (in less than 10 s). All analyzed cells were well isolated from the bulk of the cell culture.

2.6. LTRS protocol with Raman characterization with 785 nm excitation

E. coli cells were cultivated for 2 hours with shaking at 37°C in CASO broth with (+) and without (-) 2 mg/L cefotaxime added to the medium. The cells were centrifuged for 4 min at 5000× g, supernatant discarded, and the pellet washed with 1ml of cold PBS three times before the LTRS measurement in order to remove any interfering Raman signal from the cultivation medium. Both the optical trapping and Raman excitation was realized with 785 nm laser beam. Acquisition was 15 accumulations of 15 s integrations (225s total integration time per sample). Laser tweezers Raman spectroscopy (LTRS) from *E. coli* cells was performed on max. 5 trapped cells for a single Raman measurement. The assessment of the cell number was based on the size of the Airy disk (800 nm). The spectra were normalized at 1004 cm^{-1} (phenylalanine). The cells were loaded into a microchamber and the specimen was placed on the piezo-stage of the LTRS system. The cells were optically trapped approximately 20 μm above the glass-liquid interface and spectrographed. The full axial extent (depth) z of the excitation region was calculated to be approximately 4 μm. This value is

comparable with the diffraction limit expected for focusing λ = 785 nm light with an NA = 1.2 microscope objective in water. The full lateral extent (width) of the excitation region therefore reaches the diffraction-limited value $\Delta x = 1.22\lambda/NA \sim 0.8$ μm. Considering that the bacterial cells are on the same order of magnitude in diameter, we assume that only a few cells (from 1 to about 5) are trapped and analyzed in the trapping region of 0.8 μm [24]. The cells were observed by a standard CCD camera through the flipping mirror FM (Fig. 1). During the acquisition of the Raman spectrum, the flipping mirror FM was flipped down and the sample illumination was switched off.

2.7. Raman spectroscopic characterization of E. coli *in the bulk with 532nm excitation*

Additional Raman spectroscopic measurements without optical trapping were realized with Renishaw In Via Raman microspectrometer with excitation at 532 nm, 100% power (approx. 150 mW at the sample plane), 20× objective and 30 accumulations of 1s for each spectrum. Cells of *E. coli* 683 were prepared as in section 2.6. The cell pellet was used to record bulk Raman spectra which served as a reference to the LTRS experiment.

2.8. Processing and analysis of Raman spectral data

In order to extract quantitative information from the acquired spectra which contain fluorescence along with the Raman signal, we adopted the high-pass signal filter (Rolling Circle Filter–RCF) [32] to separate narrow Raman spectral peaks from the wide spectral background. With an appropriate choice of the filter parameters (filter width and number of filter passes) the background can be effectively removed with no significant distortion of the signal peaks. We kept the same filter parameters for all the measurements presented in this paper. Principal component analysis (PCA) was used for analysis of the obtained Raman spectra. The PCA analysis and RCF were both realized via a homebuilt Raman analysis toolkit based on Matlab (MathWorks, Natick, MA, USA).

3. Results and discussion

3.1. Optical trapping in microfluidic environment

We transported the bacterial cells with optical tweezers into the chambers, see Figure 4. Effectiveness of single particle micromanipulation depended on the concentration of the particles in the channel. Optimal single cell micromanipulation was effective only in highly diluted cell suspensions, see Figure 4 and Figure 5.

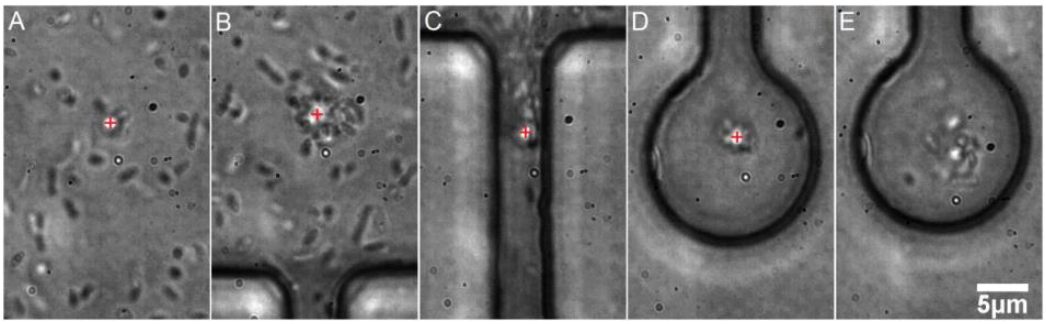

Figure 4. Demonstration of optical trapping and transport of multiple *E. coli* cells from the main microfluidic channel into the microchamber. The position of optical trap is visible as a bright spot near the centers of the images A-D, and it is also marked by a red plus sign for clarity. A: The optical trap is switched on and a few bacteria are trapped almost immediately. B: The microscope table is operated so that the optical trap is moved towards the neck, dragging with it a swarm of bacterial cells. C: The optical trap passes through the narrow neck, losing some of the trapped cells in the process. D: The optical trap is in the microchamber and it contains several cells. E: The optical trap is switched off and the cells disperse in the chamber. It is possible to regulate the amount of trapped

bacteria by a proper dilution of the culture in the main channel. We were able to easily load individual bacteria into separate chambers, see Figure 5.

3.2. *Time lapse observation of* E. coli *growth in microchambers under antibiotic stress*

The microchamber chip design was used for time-lapse visual and spectroscopic observations of individual cells, in a similar manner as in our previous experiments [19], see Figure 5. The cells were loaded in the microfluidic chambers and the chip was perfused with CASO broth containing 2 mg/L cefotaxime. The cells have elongated about 5 times during the 60 minutes of microfluidic cultivation. This phenomenon was observed previously [33]. Some cephalosporin antibiotics exhibit this effect in certain range of concentrations since they impair the process of cell division in the sensitive cells [33].

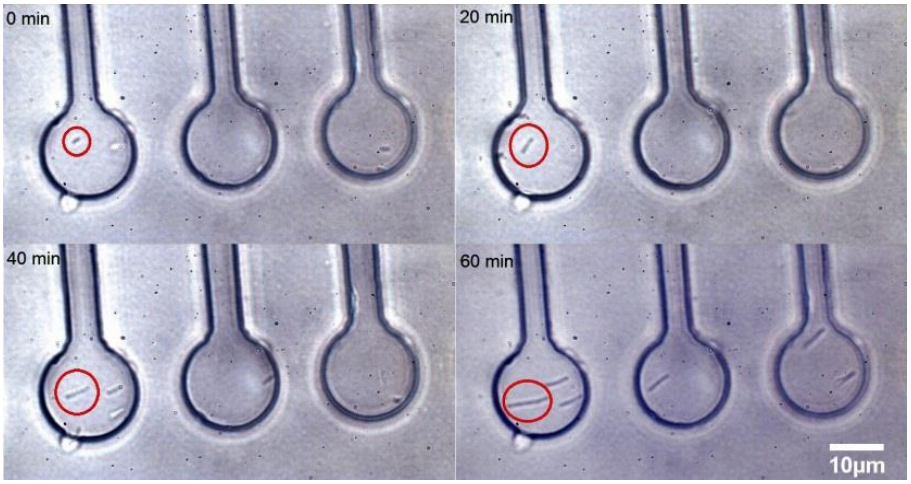

Figure 5. A time-lapse sequence of growing *E. coli* cells in microchambers in presence of 2 mg/L cefotaxime in CASO medium introduced by a syringe pump into the CASO medium running through the microfluidic chip. Red circle shows an individual bacterium growing over time. The time of cultivation in minutes is given for each quadrant in the top left corner. These bacterial cells were individually loaded into the chambers by optical tweezers. The cells became progressively longer over time in response to the cefotaxime treatment. The red circled bacterium has elongated about 5 times during the 60 minutes of microfluidic cultivation. Scale bar: 10 µm.

3.3. *Experiments with LTRS of* E. coli *cells with 785 nm wavelength for trapping and Raman excitation*

We collected Raman spectra of the optically trapped *E. coli* cultivated for 2 hours with shaking at 37 °C in CASO broth with (+) and without (-) 2 mg/L cefotaxime added to the medium, see Figure 6. The peaks at 855, 1126, 1236, 1340, 1449, and 1551 cm^{-1} decreased with exposition to cefotaxime, while the peaks at 1100, and 1653 cm^{-1} increased with cefotaxime present. We identified all the major peaks and compared their wavenumbers to a reference [11], see table 1. We tried to discriminate between the (+) and (-) group with the PCA method. The PCA from the spectra of *E. coli* presented on Figure 6 is depicted on Figure 7. The difference between the (+) and (-) group was highly statistically significant. These data cannot be directly compared with the Raman measurements of *E. coli* at 532 nm, since the relative peak intensities are rather different with the two excitation wavelengths.

Preprints (www.preprints.org) | NOT PEER-REVIEWED | Posted: 12 April 2018 doi:10.20944/preprints201804.0163.v1

Peer-reviewed version available at Sensors 2018, 18, 1623; doi:10.3390/s18051623

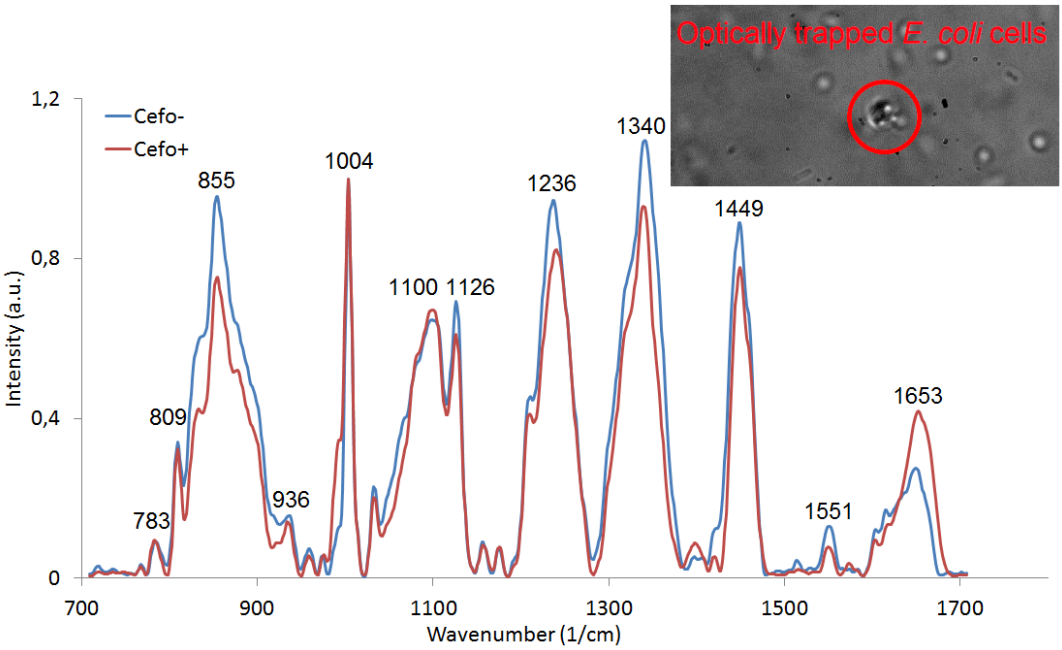

Figure 6. Raman spectra of optically trapped *E. coli* cells cultivated with (+) and without (-) cefotaxime added to the medium. Each spectrum was averaged from 16 (+) and 9 (-) spectra. The spectra show several peaks typical for bacteria, all the major peaks were identified, see Table 1. The inset shows a bright field image of the trapped bacteria prepared for spectroscopic measurement. The red circle defines the optical trap location.

Table 1. Raman peaks of *E. coli* cells and their assignments.

Wavenumber (1/cm)[1]	Assignment	Wavenumber (1/cm)	Assignment
728 (719, 723)	Adenine	1095 (1100, 1094)	DNA: OPO^-
783 (783, 783)	Nucleic acids (C, T)	1126 (1126, 1126)	C-N, C, T
813 (809, 810)	Tyrosine	1257 (1236, 1244)	Amide III
857 (855, 853)	Tyrosine	1340 (1340, 1337)	Nucleic acids (A, G)
936 (936, 934)	DNA backbone	1453 (1449, 1454)	C-H_2 def., lipids
1004 (1004, 1001)	Phenylalanine	1660 (1653, 1655)	Amide I

[1] Wavenumbers from [11] (633 nm excitation) are presented first (black), the numbers in bracket represent our measurements taken at 785 nm (red) and 532 nm (green) excitation wavelength.

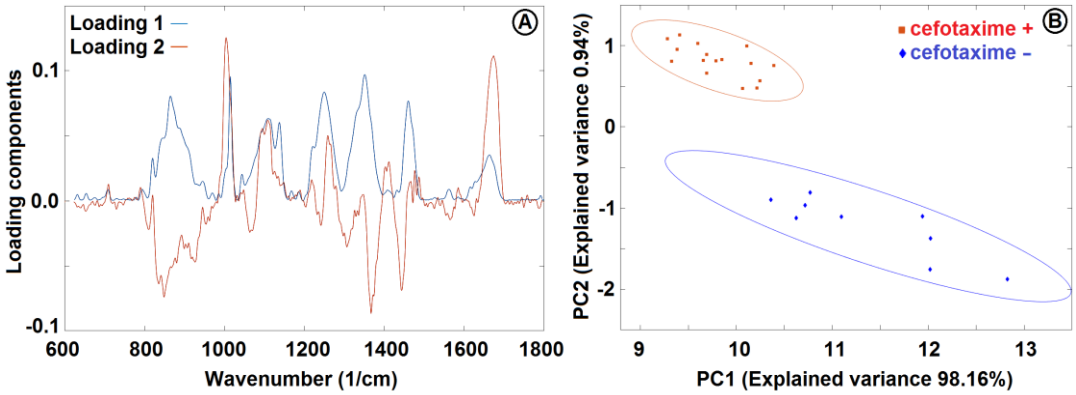

Figure 7. PCA loadings (A) and PCA analysis (B) of *E. coli* cultivated in CASO broth with and without 2 mg/L cefotaxime added to the medium. See Figure 6 for the Raman spectra and section 2.6 for sample treatment details. PC1 and PC2 were used for discrimination between the cells with (+) and without (-) cefotaxime. The ellipsoids represent 95% probability level.

Preprints (www.preprints.org) | NOT PEER-REVIEWED | Posted: 12 April 2018 doi:10.20944/preprints201804.0163.v1

Peer-reviewed version available at Sensors 2018, 18, 1623; doi:10.3390/s18051623

3.4. Raman microspectroscopy of E. coli cells with 532 nm excitation

We used commercial Raman microspectrometer Renishaw In Via to obtain spectra from *E. coli* cells cultivated in CASO broth with (+) and without (-) cefotaxime, with excitation wavelength 532 nm, see Figure 8. We identified the dominant peaks, see Table 1. The spectrum of pure *E. coli* samples includes the peaks around 1458 cm^{-1} and 1485 cm^{-1} (in our case this was precisely 1454 cm^{-1} and 1482 cm^{-1}), which were identified by Kirchhoff et al. [16] as a promising indicator of drug induced changes in *E. coli*. We can see that our results agree with these findings: the 1482 cm^{-1} peak intensity tends to decrease with the presence of cefotaxime relative to the 1454 cm^{-1} peak. Additionally, we have identified in our data and those of Kirchhoff et al. [16] that peak intensity at 783 cm^{-1} invariably decreased in the presence of the antibiotic relatively to the 1001 cm^{-1} signal of phenylalanine. The bar graphs representing the ratios of these peaks are depicted in Figure 9. We further supported our findings with PCA analysis, see Figure 10. PCA analysis was capable of resolving the cells grown with (+) and without (-) cefotaxime with high reliability.

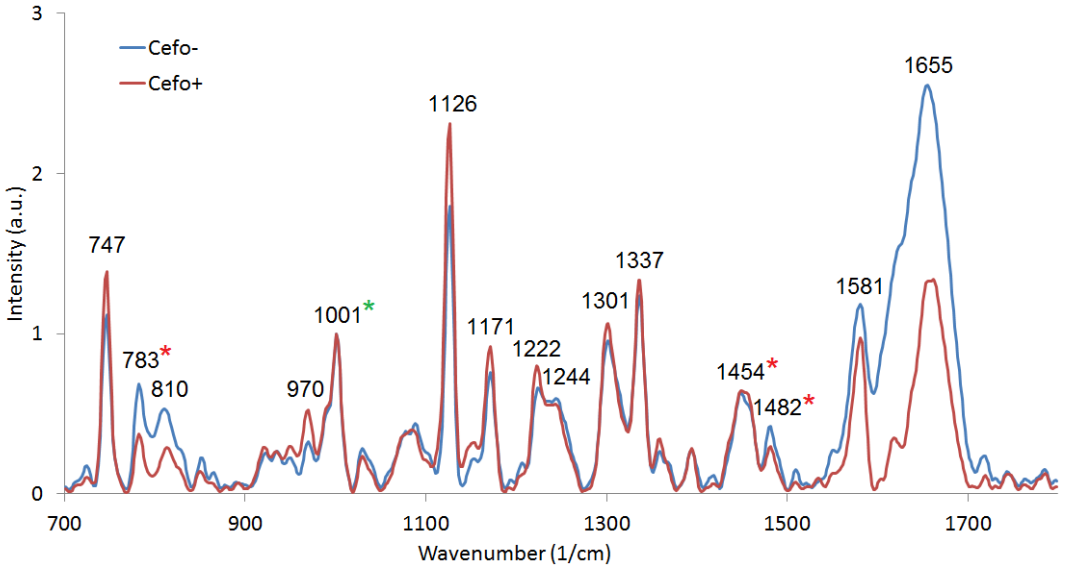

Figure 8. Raman spectra of *E. coli* cells cultivated for 3h in CASO broth with (+) and without (-) cefotaxime, washed with PBS. Averaged from 10 (+) and 6 (-) spectra. Measured at Renishaw In Via with excitation at 532 nm, 100% power, 20x objective and 30s integration, normalized at 1001 cm^{-1}. The normalization peak was highlighted in the spectrum by a green asterisk (*). Red asterisks (*) denote the peaks which were selected for further analysis, see text.

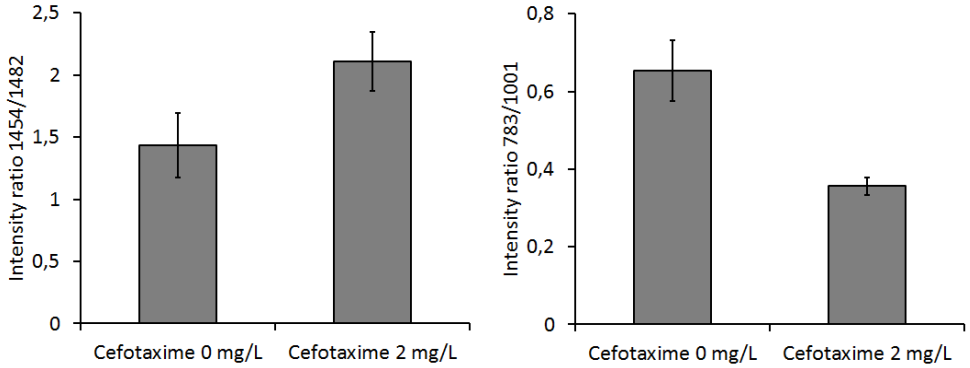

Figure 9. Ratios of Raman peaks for cells cultivated with (2 mg/L) and without (0 mg/L) cefotaxime: 1454/1482 cm^{-1} and 783/1001 cm^{-1}. The differences in peak ratios for the experimental and control group were statistically significant. The error bars represent 2 SD.

Preprints (www.preprints.org) | NOT PEER-REVIEWED | Posted: 12 April 2018 doi:10.20944/preprints201804.0163.v1

Peer-reviewed version available at Sensors 2018, 18, 1623; doi:10.3390/s18051623

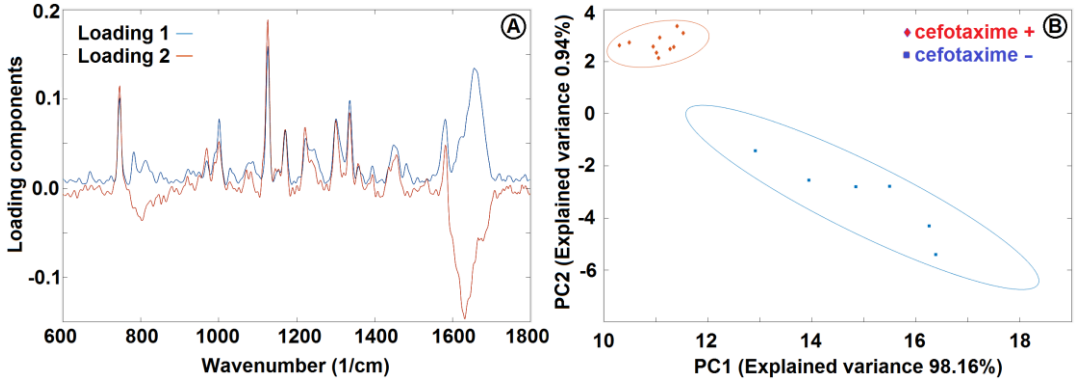

Figure 10. PCA loadings (A) and PCA analysis (B) of *E. coli* cultivated in CASO broth with and without 2 mg/L cefotaxime added to the medium. See Figure 8 for the Raman spectra and section 2.7 for sample treatment details. PC1 and PC2 were used for discrimination between the cells with (+) and without (-) cefotaxime. The ellipsoids represent 95% probability level.

4. Conclusions

Optical trap and a microchamber based optofluidic system allowed us to effectively isolate the individual bacterial cells of *E. coli* and observe the changes of morphology induced by cephalosporin antibiotic cefotaxime. The system proved to be the ideal combination for simple non-contact micromanipulation of individual cells and their cultivation in a highly controlled environment with the possibility of time-lapse recording of their morphology and development. Based on Raman spectra of optically trapped cells of *E. coli*, we were able to discriminate by PCA between the cells stressed by cefotaxime and the control cultivated in pure CASO broth. We also identified several peaks which changed their magnitude with varying exposure of the cells to cefotaxime. These measurements were realized with 785 nm Raman excitation and trapping wavelength. Raman microspectroscopy of bacterial samples at 532 nm provided us with spectra that are complementary to the measurements at 785 nm. These data independently support the finding of Kirchhoff et al. [16], that the ratio of the peaks at 1458 cm^{-1} and 1485 cm^{-1} changes with drug concentration in the medium. We identified and assigned all the major Raman peaks typical for *E. coli* according to a reference [11]. The intensity of peaks and its relative intensity changes were different in the spectra recorded at 785 nm and 532 nm excitation.

We present this work as a proof of principle that our approach combining microfluidic chambers with LTRS provides a solid optofluidic platform for single cell manipulation and analysis by optical microscopy and Raman spectroscopy. In order to design novel microfluidic chip for bacterial separation and identification from different body fluids, such as sputum, blood, or urine, we will exploit LTRS in connection with different microfluidic techniques based e.g. on centrifugal force, dielectrophoresis, microfiltration, flow-focusing, surface acoustic wave, etc. to sort and cultivate cells in microchambers. We are aiming for an advanced connection of microfluidics and optical trapping for analysis of bacteria which would enable fast and accurate determination of bacterial sepsis.

Acknowledgments: We thank the staff at the Institute for Medical Microbiology at the Jena University Hospital for the collaboration. The research was supported by GACR GA16-12477S, Ministry of Education, Youth and Sports of the Czech Republic (project LO1212). The research infrastructure was funded by Ministry of Education, Youth and Sports of the Czech Republic and European Commission (project CZ.1.05/2.1.00/01.0017) and by the Czech Academy of Sciences (project RVO:68081731). U.N. and J.K. acknowledge funding from the BMBF via the CSCC (FKZ 01EO1502) and Research Campus InfectoGnostics (FKZ 13GW0096F). This article is based upon work from COST Action "Raman-based applications for clinical diagnostics - Raman4Clinics" (BM 1401), supported by COST (European Cooperation in Science and Technology). Financial support from the DFG via the Jena Biophotonic and Imaging Laboratory (JBIL, FKZ PO 633/29-1, BA 1601/10-1) is highly acknowledged.

Author Contributions: Z.P. conceived and performed the experiments, analyzed the results and wrote the article. S.B. designed and built the experimental apparatus, performed the experiments and analyzed data; J.J. co-designed and manufactured the microfluidic chips; J.K. and U.N. conceived the experiments, prepared together with A.T. the cells and co-wrote the article; O.S. conceived the experiments, coordinated the project and secured the financial support; P.Z. provided consultations and secured the infrastructural and financial support.

Conflicts of Interest: The authors declare no conflict of interest.

References

[1] Liberale, C.; Cojoc, G.; Bragheri, F.; Minzioni, P.; Perozziello, G.; La Rocca, R.; Ferrara, L.; Rajamanickam, V.; Di Fabrizio, E.; Cristiani, I. Integrated microfluidic device for single-cell trapping and spectroscopy. *Sci. Rep.* **2013**, *3*, 1–6, doi: 10.1038/srep01258.

[2] Redding, B.; Schwab, M. J.; Pan, Y. Review: Raman spectroscopy of optically trapped single biological micro-particles. *Sensors* **2015,** *15,* 19021–19046, doi:10.3390/s150819021.

[3] Gilany, K.; Moazeni-Pourasil, R. S.; Jafarzadeh, N.; Savadi-Shiraz, A. Metabolomics fingerprinting of the human seminal plasma of asthenozoospermic patients. *Mol. Reprod. Dev.* **2014,** *81,* 84–86, doi: 10.1002/mrd.22284.

[4] Wang, S. Y.; Hasty, C. E.; Watson, P. A.; Wicksted, J. P.; Stith, R. D.; March, W. F. Analysis of metabolites in aqueous solutions by using laser Raman spectroscopy. *Appl. Opt.* **1993**, *32,* 925–929, doi: 10.1364/AO.32.000925.

[5] Rösch, P.; Harz, M.; Schmitt, M.; Peschke, K.-D.; Ronneberger, O.; Burkhardt, H.; Motzkus, H.-W.; Lankers, M.; Hofer, S.; Thiele, H.; Popp, J. Chemotaxonomic identification of single bacteria by micro-Raman spectroscopy: Application to clean-room-relevant biological contaminations. *Appl. Environ. Microbiol.* **2005,** *71,* 1626–1637, doi: 10.1128/AEM.71.3.1626-1637.2005.

[6] Willemse-Erix, D. F. M.; Scholtes-Timmerman, M. J.; Jachtenberg, J.-W.; van Leeuwen, W. B.; Horst-Kreft, D.; Schut, T. C. B.; Deurenberg, R. H.; Puppels, G. J.; van Belkum, A.; Vos, M. C.; Maquelin, K. Optical fingerprinting in bacterial epidemiology: Raman spectroscopy as a real-time typing method. *Clin. Microbiol.* **2009,** *47,* 652–659, doi: 10.1128/JCM.01900-08.

[7] Stöckel, S.; Kirchhoff, J.; Neugebauer, U.; Rösch, P.; Popp, J. The application of Raman spectroscopy for the detection and identification of microorganisms. *J. Raman Spectrosc.* **2016,** *47,* 89–109, doi: 10.1002/jrs.4844.

[8] Xie, C.; Goodman, C.; Dinno, M. A.; Li, Y. Q. Real-time Raman spectroscopy of optically trapped living cells and organelles. *Opt. Express* **2004,** *25,* 6208–6214, doi: 10.1364/OPEX.12.006208.

[9] Xie, C.; Chen, D.; Li, Y.-Q. Raman sorting and identification of single living micro-organisms with optical tweezers. *Opt. Lett.* **2005,** *30,* 1800–1802, doi: 10.1364/OL.30.001800.

[10] Neuman, K. C.; Chadd, E. H.; Liou, G. F.; Bergman, K.; Block, S. M. Characterization of photodamage to *Escherichia coli* in optical traps. *Biophys. J.* **1999,** *77,* 2856–2863, doi: 10.1016/S0006-3495(99)77117-1.

[11] Chan, J. W.; Winhold, H.; Corzett, M. H.; Ulloa, J.; Cosman, M.; Balhorn, R.; Huser, T. Monitoring dynamic protein expression in living *E. coli* bacterial cells by laser tweezers Raman spectroscopy. *Cytometry Part A* **2007,** *71A,* 468–474, doi: 10.1002/cyto.a.20407.

[12] Dai, J.; Hamon, M.; Jambovane, S. Microfluidics for antibiotic susceptibility and toxicity testing. *Bioengineering* **2016,** *3,* 25, doi: 10.3390/bioengineering3040025.

[13] Assmann, C.; Kirchhoff, J.; Beleites, C.; Hey, J.; Kostudis, S.; Pfister, W.; Schlattmann, P.; Popp, J.; Neugebauer, U. Identification of vancomycin interaction with *Enterococcus faecalis* within 30 min of interaction time using Raman spectroscopy. *Anal. Bioanal. Chem.* **2015,** *407,* 8343–8352, doi: 10.1007/s00216-015-8912-y.

[14] Schröder, U.; Kirchhoff, J.; Hübner, U.; Mayer, G.; Glaser, U.; Henkel, T.; Pfister, W.; Fritzsche, W.; Popp, J.; Neugebauer:, U. On-Chip spectroscopic assessment of microbial susceptibility to antibiotics within 3½ hours. *J. of Biophotonics*, **2017,** *10,* 1547–1557, doi: 10.1002/jbio.201600316.

[15] Schröder, U.-C.; Beleites, C.; Assmann, C.; Glaser, U.; Hübner, U.; Pfister, W.; Fritzsche, W.; Popp, J.; Neugebauer, U. Detection of vancomycin resistances in enterococci within 3½ hours. *Sci. Rep.* **2015,** *5,* 8271, doi: 10.1038/srep08217.

[16] Kirchhoff, J.; Glaser, U.; Bohnert, J. A.; Pletz, M.; Popp, J.; Neugebauer, U. Simple ciprofloxacin resistance test and determination of minimal inhibitory concentration (MIC) within two hours using Raman spectroscopy. *Anal. Chem.* **2018,** *90,* 1811–1818, doi: 10.1021/acs.analchem.7b03800.

[17] Schröder, U.-C.; Ramoji, A.; Glaser, U.; Sachse, S.; Leiterer, C.; Cszaki, A.; Huebner, U.; Fritzsche, W.; Pfister, W.; Bauer, M.; Popp, J.; Neugebauer, U. Combined dielectrophoresis-Raman setup for the classification of pathogens recovered from the urinary tract. *Anal. Chem.* **2013,** *85,* 10717–10724, doi: 10.1021/ac4021616.

[18] Schröder, U.-C.; Bokeloh, F.; O'Sullivan, M.; Glaser, U.; Wolf, K.; Pfister, W.; Popp, J.; Ducreé, J.; Neugebauer, U. Rapid, culture-independent, optical diagnostics of centrifugally captured bacteria from urine samples. *Biomicrofluidics* **2015,** *9,* 044118, doi: 10.1063/1.4928070.

[19] Pilát, Z.; Jonáš, A.; Ježek, J.; Zemánek, P. Effects of infrared optical trapping on *Saccharomyces cerevisiae* in a microfluidic system. *Sensors* **2017,** *17,* 2640, doi: 10.3390/s17112640.

[20] Jonáš, A.; Pilát, Z.; Ježek, J.; Bernatová, S.; Fořt, T.; Zemánek, P.; Aas, M.; Kiraz, A. Thermal tuning of spectral emission from optically trapped liquid-crystal droplet resonators. *JOSA B* **2017,** *34,* 1855–1864, doi: 10.1364/JOSAB.34.001855.

[21] Samek, O.; Jonáš, A.; Pilát, Z.; Zemánek, P.; Nedbal, L.; Tříska, J.; Kotas, P.; Trtílek, M. Raman Microspectroscopy of individual algal cells: sensing unsaturation of storage lipids *in vivo*. *Sensors* **2010,** *10,* 8635–8651, doi: 10.3390/s100908635.

[22] Pilát, Z.; Bernatová, S.; Ježek, J.; Šerý, M.; Samek, O.; Zemánek, P.; Nedbal, L.; Trtílek, M. Raman microspectroscopy of algal lipid bodies: beta-carotene as a sensor. *SPIE Proc.* **2011,** *8306,* 83060L:1–7, doi: 10.1117/12.912264.

[23] Pilát, Z.; Bernatová, S.; Ježek, J.; Šerý, M.; Samek, O.; Zemánek, P.; Nedbal, L.; Trtílek, M. Raman microspectroscopy of algal lipid bodies: beta-carotene quantification. *J. Appl. Phycol.* **2012,** *24,* 541–546, doi: 10.1007/s10811-011-9754-4.

[24] Bernatová, S.; Samek, O.; Pilát, Z.; Šerý, M.; Ježek, J.; Jákl, P.; Šiler, M.; Krzyžánek, V.; Zemánek, P.; Holá, V.; Dvořáčková, M.; Růžička, F. Following the mechanisms of bacteriostatic versus bactericidal action using Raman spectroscopy. *Molecules* **2013,** *18,* 13188–13199, doi: 10.3390/molecules181113188.

[25] Samek, O.; Mlynáriková, K.; Bernatová, S.; Ježek, J.; Krzyžánek, V.; Šiler, M.; Zemánek, P.; Růžička, F.; Holá, V.; Mahelová, M. *Candida parapsilosis* biofilm identification by Raman spectroscopy. *Int. J. Mol. Sci.* **2014,** *15,* 23924–23935, doi: 10.3390/ijms151223924.

[26] Samek, O.; Bernatová, S.; Ježek, J.; Šiler, M.; Šerý, M.; Krzyžánek, V.; Hrubanová, K.; Zemánek, P.; Holá, V.; Růžička, F. Identification of individual biofilm-forming bacterial cells using Raman tweezers. *J. Biomed. Opt.* **2015,** *20,* 051038, doi: 10.1117/1.JBO.20.5.051038.

[27] Mlynáriková, K.; Samek, O.; Bernatová, S.; Růžička, F.; Ježek, J.; Hároniková, A.; Šiler, M.; Zemánek, P.; Holá, V. Influence of culture media on microbial fingerprints using Raman spectroscopy. *Sensors* **2015,** *15,* 29635–29647, doi: 10.3390/s151129635.

[28] Petrov, D. V. Raman spectroscopy of optically trapped particles. *J. Opt. A: Pure Appl. Opt.* **2007,** *9,* 139–156, doi: 10.1088/1464-4258/9/8/S06.

[29] Jonáš, A.; Zemánek, P. Light at work: The use of optical forces for particle manipulation, sorting, and analysis. *Electrophoresis* **2008,** *29,* 4813–4851. 10.1002/elps.200800484.

[30] Xia, Y.; Whitesides, G. M. Soft lithography. *An. Rev. Mat. Sci.* **1998,** *28,* 153–184, doi: 10.1146/annurev.matsci.28.1.153.

[31] Pilát, Z.; Ježek, J.; Šerý, M.; Trtílek, M.; Nedbal, L.; Zemánek, P. Optical trapping of microalgae at 735–1064 nm: Photodamage assessment. *J. Photochem. Photobiol. B: Biology*, **2013,** *121,* 27 – 31, doi: 10.1016/j.jphotobiol.2013.02.006.

[32] Brandt, N. N.; Brovko, O. O.; Chikishev, A. Y.; Paraschuk, O. D. Optimization of the Rolling-Circle Filter for Raman Background Subtraction. *Appl. Spectrosc.* **2006,** *60,* 288–293, doi: 10.1366/000370206776342553.

[33] Choi, J.; Yoo, J.; Lee, M.; Kim, E.-G.; Lee, J. S.; Lee, S.; Joo, S.; Song, S. H.; Kim, E.-C.; Lee, J. C.; Kim, H. C.; Jung, Y.-G.; Kwon, S. A rapid antimicrobial susceptibility test based on single-cell morphological analysis. *Sci. Transl. Med.* **2014,** *6,* 267ra174, doi: 10.1371/journal.pone.0148864.